Aligning microcavity resonances in silicon photonic-crystal slabs using laser-pumped thermal tuning

Jun Pan,[1,a)] Yijie Huo,[1] Kazuhiko Yamanaka,[1,2] Sunil Sandhu,[3] Luigi Scaccabarozzi,[1] Rolf Timp,[3] Michelle L. Povinelli,[3] Shanhui Fan,[3] M. M. Fejer,[3] and James S. Harris[1]
[1]*Solid State and Photonics Laboratory, Stanford University, Stanford, California 94305, USA*
[2]*Semiconductor Device Research Center, Semiconductor Company, Matsushita Electric Industrial Co., Ltd., Osaka 569-1193, Japan*
[3]*E.L. Ginzton Laboratory, Stanford University, Stanford, California 94305, USA*

(Received 30 January 2008; accepted 22 February 2008; published online 12 March 2008)

We report the postfabrication alignment of multiple microcavity resonances in silicon photonic-crystal (PhC) slabs using laser-pumped thermal tuning. The thermal gradient resulting from a focused laser spot was used to differentially tune the resonant wavelengths of two microcavities spaced about 50 μm apart. The resonant wavelengths could be brought closer together, over a tunable range of more than 5 nm. A cross over in the resonant wavelengths was demonstrated, showing that two microcavities can be tuned to the identical wavelength. The results show that differential thermal tuning can be used to remove slight fabrication differences in nominally identical microcavities, relaxing the fabrication tolerances that will be required to realize coupled-resonator structures in PhCs. © *2008 American Institute of Physics*.
[DOI: 10.1063/1.2896615]

Photonic-crystal (PhC) structures incorporating multiple microcavities are predicted to exhibit a wide range of useful optical functionalities. Two-cavity designs, for example, can be tailored to give all-pass,[1] bandpass,[2] flat-top,[2] or channel-drop[3] filter response. Coupled multicavity structures have further been proposed for the slowing[1,4] and stopping[5,6] of light. However, an important prerequisite for the experimental demonstration of any of these schemes is the ability to tune different microcavities to a desired resonance frequency. Due to slight geometrical errors introduced during the fabrication process, it is generally not possible to fabricate two PhC microcavities with identical resonances. Previous work has demonstrated thermal tuning of a single microcavity[7,8] or aligning the resonant frequency of a single microcavity to a quantum dot[9] in PhC structures. In this paper, we demonstrate the use of differential thermal tuning to align the resonance frequencies of two microcavities in PhC structures, eliminating the effect of fabrication error.

The thermal tuning technique requires no extra materials or structures, which avoids the potential quality degradation of the PhC microcavities and excess fabrication complexity. Furthermore, we directly measure device transmission in our experiments rather than measuring the light emitted out of the PhC plane as in some previous works.[7,9] Transmission measurements are particularly relevant in the context of on-chip, integrated optics applications, where the ultimate goal is to integrate multiple or cascaded devices. For instance, Xu *et al.*[10] have demonstrated that differential thermal tuning can be used to tune the transmission line shape of silicon microresonator devices yielding adjustable optical delays.

We used a silicon-membrane PhC structure with a triangular lattice of airholes. Figure 1(a) shows a scanning electron micrograph (SEM) of the device. The silicon membrane was 0.32 μm thick, the hole diameter was 232 nm, and the nearest-neighbor hole separation (lattice constant) was 386 nm. A single-line-defect (W1) waveguide was formed by removing one row of holes. Away from the central region, the W1 waveguide was coupled to a lower-loss strip waveguide. Two microcavities C1 and C2 were placed on opposite sides of the central waveguide region. Each microcavity was formed by five missing holes, with the nearest hole on either side shifted outward by 77 nm ($0.2a$) to increase the intrinsic (radiation) quality factor Q_{rad}.[11] The waveguide-resonator coupling occurs through a barrier of three rows of holes. The diameters of holes along the waveguide and the six holes along the side of the resonator closest to the waveguide are reduced to 204 nm in order to facilitate waveguide-cavity coupling.[12] The center-to-center separation of the microcavities was about 54 μm in the horizontal direction and each microcavity was separated from the waveguide by three rows of holes. Under the SEM, the two microcavities appear identical.

Devices were fabricated in the Stanford Nanofabrication Facility, on silicon-on-insulator Unibond wafers manufactured by SOITEC with a 1 μm buried oxide layer. The strip waveguides and PhC were patterned in polymethyl methacrylate e-beam resist by electron beam lithography in a Raith 150 system. The pattern was then transferred to a 150 nm SiO_2 layer (deposited by low pressure chemical vapor deposition before lithography) using reactive ion etching with $CF_4/CHF_3/Ar$ chemistry. The oxide layer served as a hard mask in the subsequent silicon etch with a combination of $HBr/NF_3/He/O_2$. Another layer of SiO_2 was deposited on the wafer with a thickness comparable to that of the buried oxide by low pressure chemical vapor deposition, followed by a step of thermal annealing at 1100 °C. We selectively etched the oxide above and below the PhC region to form an air-bridged slab, while letting the oxide around the strip waveguide remain as cladding. A gold mask with a chromium adhesion layer, formed by a procedure of optical lithography, metal evaporation, and lift-off, was used to protect the oxide cladding around the strip waveguide against hydrofluoric acid. Finally, the devices were diced from the wafers and the waveguide input and output facets were polished to mirror surfaces in order to facilitate the transmission

a)Electronic mail: panjun@stanford.edu.

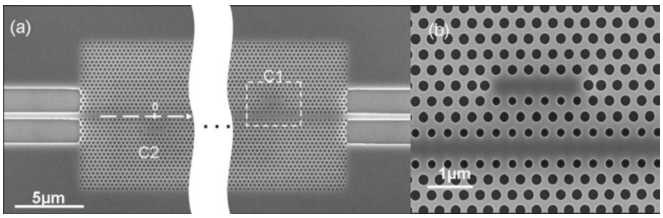

FIG. 1. SEM images of the fabricated device. (a) Top view of the PhC structure with two cavities. (b) Magnified view of microcavity C1.

measurement. The total length of the waveguide is about 1.2 mm while the PhCs are in a region smaller than $100 \times 12\ \mu m^2$.

The transmission measurements were performed using a tunable laser source. TE-polarized light (in-plane polarization) was injected into the edge of the waveguide using an objective lens with numerical aperture of 0.65. The emitted light from the far edge of the device was collected by a second objective lens and the power was measured using a germanium detector.

To tune the microcavity resonance wavelengths, an Ar ion, cw pump laser with a wavelength of 488 nm was used. The pumping laser was focused onto the surface of the PhC from the perpendicular (vertical) direction, using an objective lens combined with a charge-coupled device camera. An optical fiber was used to guide the laser from the laser source into the objective lens. The spot size of the pumping laser is $\sim 2\ \mu m$ in diameter. The focused laser spot induces a thermal gradient in the suspended silicon membrane, which shifts the local refractive index (n) by a different amount at each cavity. For silicon, $\Delta n/\Delta T$ is $1.85 \times 10^{-4}/K$ at 1.55 μm,[13] and a temperature difference of 10 K between the cavities will result in an index difference of roughly 0.002. Since the resonance wavelength of each cavity shifts by an amount proportional to the local refractive index ($\Delta\lambda/\lambda \approx \Delta n/n$), the thermal gradient can be used to differentially tune the two resonances.

For a single cavity coupled to a waveguide, the expected transmission spectrum has a Lorentzian dip at the resonance wavelength. For two cavities, the spectrum changes qualitatively as a function of the detuning between the cavity resonances and the relative phase of the cavities. From coupled-mode theory, the general expression for the transmitted power is[14,15]

$$|T(\lambda)|^2 = \left(\frac{|t_1 t_2|}{1-|r_1 r_2|}\right)^2 \frac{1}{1+4\left(\frac{\sqrt{|r_1 r_2|}}{1-|r_1 r_2|}\right)^2 \sin^2\theta}. \quad (1)$$

t_1 and t_2 are complex transmission coefficients for resonators 1 and 2, respectively, given by

$$t_i = \frac{j(\omega-\omega_i)+\gamma}{j(\omega-\omega_i)+(\gamma_c+\gamma)}, \quad (2)$$

where ω_i is the resonant frequency of resonator 1 or 2. Frequency and wavelength are related by $\omega = 2\pi c/\lambda$. γ is the amplitude intrinsic-loss rate, related to the intrinsic quality factor as $\gamma = \pi c/Q_{\text{int}}\lambda_0$. (The intrinsic-loss process includes both the radiation loss and material absorption loss.) γ_c is the total waveguide-cavity amplitude-coupling rate; $\gamma_c = \pi c/Q_c\lambda_0$. r_1 and r_2 are the complex reflection coefficients, given by

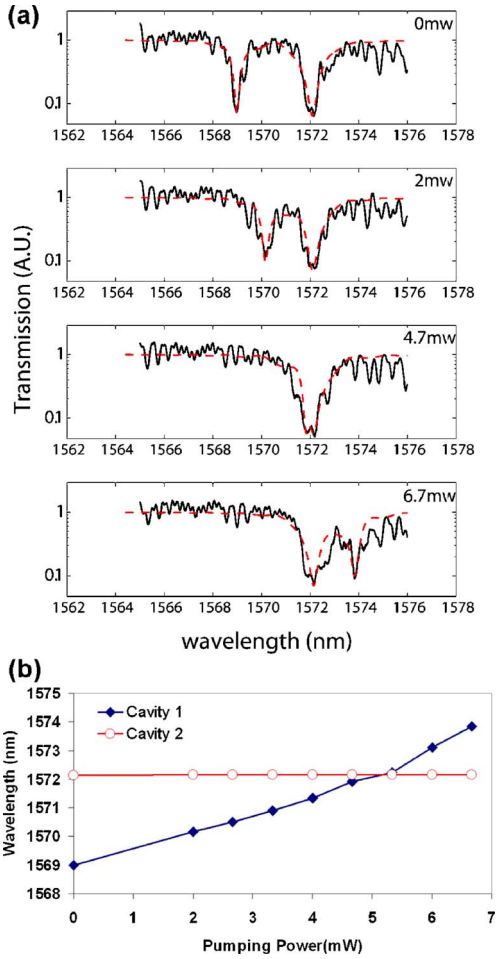

FIG. 2. (Color online) Experimental results of laser-pumped thermal tuning of PhC microcavities with laser pump light focused near microcavity C1. (a) Transmission spectra for pump powers between 0 and 6.7 mW. Solid black lines show experimental data and red dashed lines show theoretical fits. (b) Resonance wavelengths (dip positions) as a function of pump power.

$$r_i = \frac{\gamma_c}{j(\omega-\omega_i)+(\gamma_c+\gamma)}. \quad (3)$$

θ is one-half the round-trip phase accumulated in the waveguides: $\theta = \frac{1}{2}\arg[r_1 r_2 e^{-2j\beta(\omega)s}]$, where $\beta(\omega)$ is the waveguide dispersion relation and s is the separation between the cavities. When the difference between the cavity resonance wavelengths (detuning) is large compared to the single-cavity transmission linewidth (proportional to $1/Q_c$), the form of the transmission spectrum reduces to a sum of two Lorentzians.

The transmission spectrum of the fabricated device is shown by the black solid line in Fig. 2(a). The red dashed line is the theoretical fitting according to Eqs. (1)–(3), in which $\beta(\omega)$ is calculated by finite-difference time-domain simulation and s is the separation between the cavities. The resonance frequency ω_i of each cavity is chosen to be the frequency with the minimum transmission power. Q_{int} and Q_c of each cavity are obtained from fitting the experimental transmission spectrum with the theoretical formula of Eqs. (1)–(3). In the absence of the pump laser, the structure exhibits two resonances for cavities C1 and C2 at 1568.99 and 1572.14 nm [Fig. 2(a)]. Cavity C1 has Q_{int} and Q_c of 9500 and 3000, respectively, and C2 has Q_{int} and Q_c of 5000 and 1600. The difference in resonant wavelengths and quality factors can be attributed to visually imperceptible fabrication

differences between the cavities shown in Fig. 1. In our experimental devices, the difference in resonance wavelength between two cavities on the same sample was typically several nanometers. For application in filters or slow light devices, the resonances must be aligned to within their linewidths or better, which imposes strict fabrication tolerances. Introducing a postfabrication tuning method relaxes the fabrication requirements.

To tune the resonance wavelengths, the pump laser was focused on the surface of the device, in the vicinity of the microcavity C1. We avoided focusing the laser spot directly on the cavity since the pump laser introduces free carriers in the silicon slab that result in optical loss. The effect of loss on Q_{int} can be reduced by focusing the laser spot several microns from the cavity since the carrier concentration decreases with distance from the laser spot due to recombination. Figure 2(a) shows measured transmission spectra for the power delivered on the sample between 0 and 6.7 mW. The spectrum exhibits two clearly separated resonance dips. (The additional oscillations seen in the spectrum are due to Fabry–Pérot reflections from the ends of the device and do not change substantially with the laser power.) The resonance wavelengths are plotted in Fig. 2(b). As the source power is increased, one resonance linearly shifts to higher wavelength and the other stays almost the same. We can infer that the longer-wavelength resonance is from C2, which is farther from the laser focus and, thus, experiences less heating and less temperature-induced shift. From the maximum shift (4.85 nm), the temperature rise at C1 was estimated to be about 59 K. If farther detuned resonances are desired, the laser spot can be moved to C2. The larger-wavelength resonance will shift to an even larger wavelength while the resonance of C1 will stay the same. During the thermal tuning of C1, its Q_{int} decreases as power increases, due to loss, and reaches 6000 at maximum power, while its Q_c does not change significantly.

The center-to-center distance between the two microcavities can be reduced to be much smaller than that of this device. When we moved the laser spot halfway in between the two microcavities, neither resonance exhibited a significant redshift. This implies that the heat flux dissipates to a negligible level after propagating half of the distance between the microcavities. We can thus expect the same differential thermal tuning results in a device with half of the cavity-to-cavity distance. To quantify this observation, we measured the resonance redshift of the two microcavities while scanning the pump laser spot along the waveguide near C2 (along the long dashed arrow in Fig. 1). Figure 3 shows the results. The zero point of the horizontal axis corresponds to the position of C2. The closer the laser spot to C2, the larger the redshift of C2. The redshift of C1 remains negligible, as the laser spot is far away from C1. Since the thermal conductivity of silicon is much greater than that of air, the temperature distribution outside the laser spot can be approximated by the two-dimensional Laplace equation. Its solution has a $\log(r)$ dependence, where r is the distance from the laser spot, roughly consistent with the data (see inset of Fig. 3). From Fig. 3, we can also extract a characteristic length (defined as the length for which the redshift drops to $1/e$ of the maximum redshift) of about 8.5 μm. For devices with a cavity-to-cavity distance smaller than the characteristic length, the same technique is still applicable. While the cavity farther from the laser spot will exhibit an observable redshift, it will be smaller than the redshift of the resonator closer to the spot due to the thermal gradient. As the cavity-to-cavity distance is decreased, the relative redshift increases more slowly with pumping power and the cross over of the two-cavity wavelengths occurs at higher power.

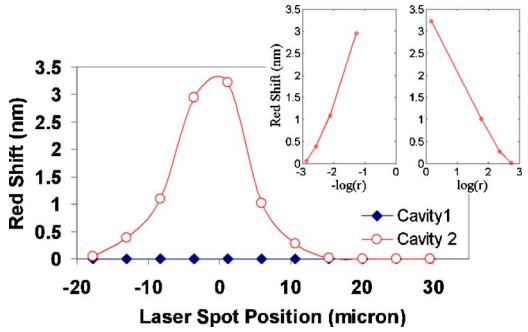

FIG. 3. (Color online) Resonance redshift of the two microcavities for different positions of the pumping laser spot. The laser spot was scanned along the waveguide near cavity 2 (along the long dashed arrow in Fig. 1), whose redshift exhibits strong dependence on the spot position. The zero of the horizontal axis corresponds to the position of cavity 2. Cavity 1 has negligible redshift due to its large distance away from the laser spot. (Inset) Redshift of cavity 2 with respect to the logarithm of the distance to laser spot.

In summary, we have experimentally demonstrated the use of laser-pumped thermal effects for differential tuning of microcavity wavelengths in silicon PhC slabs. An initial difference of 3.15 nm in the resonant wavelengths of two closely separated microcavities was decreased to zero using the thermal gradient induced by a focused laser spot. Using multiple spots should allow the postfabrication alignment of multiple microcavity resonances. This technique should be useful for the realization of increasingly complex devices employing multiple microcavities in PhC structures. Thermal tuning could be used to improve the performance of passive multicavity devices, such as filters. Moreover, combined with faster tuning methods such as free-carrier injection, dynamical reconfiguration schemes such as stopping-light systems[5,6] could be realized in PhC structures.

This work was supported in part by the Slow Light program at DARPA DSO, under the AFOSR Grant No. FA9550-05-0414 and by the Packard Foundation.

[1]Z. Wang and S. Fan, Phys. Rev. E **68**, 066616 (2003).
[2]L.-L. Lin, Z.-Y. Li, and B. Lin, Phys. Rev. B **72**, 165330 (2005).
[3]S. Fan, P. R. Villeneuve, J. D. Joannopoulos, and H. A. Haus, Phys. Rev. Lett. **80**, 960 (2003).
[4]A. Yariv, Y. Xu, R. K. Lee, and A. Scherer, Opt. Lett. **24**, 711 (1999).
[5]M. F. Yanik and S. Fan, Phys. Rev. Lett. **92**, 083901 (2004).
[6]M. F. Yanik, W. Suh, Z. Wang, and S. Fan, Phys. Rev. Lett. **93**, 233903 (2004).
[7]T. Asano, W. Kunishi, M. Nakamura, B. S. Song, and S. Noda, Electron. Lett. **41**, 37 (2005).
[8]I. Märki, M. Salt, H. P. Herzig, R. Stanley, L. El Melhaoui, P. Lyan, and J. M. Fedeli, Opt. Lett. **31**, 513 (2006).
[9]A. Faraon, D. Englund, I. Fushman, N. Stoltz, P. Petroff, and J. Vuckovic, Appl. Phys. Lett. **90**, 213110 (2007).
[10]Q. Xu, J. Shakya, and M. Lipson, Opt. Express **14**, 14 (2006).
[11]Y. Akahane, T. Asano, B. S. Song, and S. Noda, Nature (London) **425**, 944 (2003).
[12]K. H. Hwang and G. H. Song, Opt. Express **13**, 1948 (2005).
[13]G. Cocorullo, F. G. C. Della, and I. Rendina, Appl. Phys. Lett. **74**, 3338 (1999).
[14]Q. Xu, S. Sandhu, M. L. Povinelli, J. Shakya, S. Fan, and M. Lipson, Phys. Rev. Lett. **96**, 123901 (2006).
[15]L. Maleki, A. B. Matsko, A. A. Savchenkov, and V. S. Ilchenko, Opt. Lett. **29**, 626 (2004).